A realistic fMRI time series simulation with individual slice motion, geometric distortion and spin saturation effect

B. Kim[1], R. Bhagalia[2], D. Yeo[3]

[1]University of Michigan Medical School, Ann Arbor, MI, United States, [2]University of Michigan, Ann Arbor, MI, United States, [3]University of Michigan, ann Arbor, MI, United States

Introduction Validation of fMRI motion correction and analyses by statistical inference have been the focus of many publications and invoked interests in developing accurate phantom data. There has been good amount of effort by many investigators for computer-generated phantoms simulating motion artifacts, however, no phantom data include accurate account of the effect of head motion. Most data sets share a common theme that assumes no inter-slice motion during the time series acquisition. The commonly used terms, "fMRI volume", "EPI volume" or "inter-volume motion", are not appropriate for fMRI time series data acquired using multi-slice EPI, and most likely single shot sequences, in which each slice is subject to a different set of motion parameters in the presence of subject's head motion. Previously, we presented a synthetic time series data set constructed with known motion parameters affecting each slice in a time series [1]. This work describes an extended study to include geometric distortion exerted on each slice computed with varying field inhomogeneity and spin saturation effect as a result of out of plane head motion.

Methods As previously described, a mathematical fMRI time series was created using a simulated T_2–weighted MRI volume representing a standard brain atlas obtained from International Consortium of Brain Mapping (ICBM) [2]. For activation simulation, intensities of selected regions were incremented by 5%. A known set of 3D motion parameters, that are smooth in time, was applied to the ICBM's T_2–weighted MRI volume to include in-plane and out-of-plane rotations, in the range of ±8º, following the interleaved acquisition order [1]. Each slice was subject to a set of rotation angles, the subsequent geometric distortion and spin saturation effect as determined by the spin excitation history. The modified slices are stacked sequentially to form a simulated fMRI volume. The final image resolution was 1.56x1.56x6 mm in 128x128x14 matrix.

Spin saturation effect: With known motion parameters and a given TR, it is possible to track the position and time of excitation of each voxel. This timing data can then be used to calculate the magnetization at various voxel positions of the time series data at different time points. Voxel intensities are proportional to the flip angle and the magnetization component in the imaging plane. Thus the intensity corruption can be recorded in subsequent slices with respect to the initial volume. Due to the out-of-plane head motion during the image acquisition, the slice selection may include some parts of adjacent slices and results in excitation of the spins in the overlapping areas before they recover with the full TR. Since the z component of the magnetization, Mz, was not allowed to recover completely before the second excitation pulse, the tipped magnetization in the transverse plane is smaller than what is expected with the TR recovery. The intensity variation at a voxel location, which has been excited n times successfully can be computed, after some simplification (i.e., α =90º), from the expression, $I_{obvs} = I_{act}\frac{1-e^{-\Delta t_n/T1}}{1-e^{-TR/T1}}$.

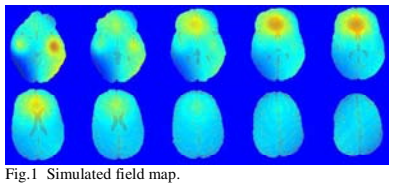

Fig.1 Simulated field map.

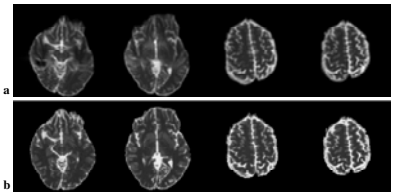

Fig.2 (a) simulated distorted EPI images and (b) corresponding T2 ICBM slices without geometric distortion.

Geometric distortion: The geometrically distorted EPI images from the simulated T2-weighted image were generated with a simulated field-map and an iterative model-based field-dependent reconstruction algorithm. [3]. The field-map was constructed using the 2D Gaussian function to create three high field regions, each of which were weighted by Gaussian in the slice direction. The three high field areas vary smoothly in the slice direction and correspond approximately to the susceptibility-induced field-inhomogeneity regions of the air-tissue interface at the sinus and frontal lobe region and the bone-tissue interface near the petrous bone at the temporal lobes. These three Gaussian shapes were added to a 3D third order polynomial to simulate additional background field-inhomogeneity. The final field-map was then normalized to values from -1 to 1 to allow for subsequent scaling for different levels of field-inhomogeneity. Fig. 1 shows the simulated field-map on the selected T2-weighted image slice locations. For the iterative reconstruction to reconstruct the distorted EPI from the undisturbed T2-w images, the k-space data $s(t_i)$ of the (distorted) images were first generated using a MR signal equation, $s(t_i) = \int_{\infty}^{\infty} f(\bar{r})e^{-j\Delta\omega(\bar{r})t_i}e^{-j2\pi(\bar{k}(t_i)\cdot\bar{r})}d\bar{r}$, where $\Delta\omega(\bar{r})$ is a spatially varying field inhomogeneity, and its discrete model. The field-map used to reconstruct $s(t)$ is updated using the motion parameters for each slice. The imaging parameters, readout time of 43.8ms and pixel bandwidth of 22.8 Hz, were used. The distorted images were then reconstructed from the k-space data. The reconstruction was achieved via the conjugate gradient algorithm that sought to minimize the quadratic penalized least squares cost function $\Psi(\mathbf{f}) = \frac{1}{2}\|\mathbf{y}-\mathbf{A}\mathbf{f}\|^2 + \frac{1}{2}\beta R(\mathbf{f})$ where β is a regularization parameter and $R(f)$ is a roughness penalty.

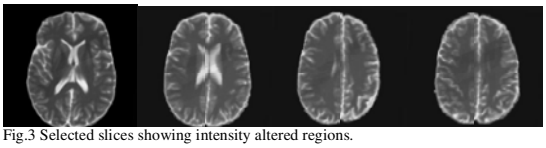

Fig.3 Selected slices showing intensity altered regions.

Results Four slices of geometrically distorted images at a simulated field-inhomogeneity level of 5ppm at 1.5T are shown in Fig. 2a and the corresponding slices of T2-w slices without geometric distortion in Fig. 2b. The areas affected by the spin saturation effect are shown in selected images as visible bands of lines separating the image intensity regions in Fig.3.

Conclusions The accuracy of motion correction algorithms for EPI time series data is difficult to assess particularly due to the lack of the truth in motion parameters and activation in human data. This study provides a more accurate test bed for the assessment of motion correction capabilities by simulating motion artifacts that include geometric distortion and intensity changes, which significantly degrade fMRI analyses. With the exception of a stationary object, i.e. physical phantom, a stack of distorted and misaligned slices cannot constitute a volume that represents the subject's head geometry, and needs to be corrected before the statistical analysis of activations in fMRI studies. This data includes motion related artifacts during the course of fMRI session that need to be addressed by algorithms used for detection and correction of motion artifacts.

References

1. Kim, et al, Proc. ISMRM 2005, p. 1555 **2**. ICBM), McGill University (www.bic.mni.mcgill.ca/brainweb/) **3**. Sutton, et al, IEEE TMI **22**, p178

Acknowledgments This research was supported in part by grant DHHS NIH 8R01 EB00309.